

Study on Mechanical and Frost Resistance Properties of Soil Solidification Rock Recycled Aggregate Concrete

Jianjun Teng, Nan Shi, Haifeng Wan*, Yangfan Xin, Cheng Jin, Jie Wang, Zuwei Liu, Huijie Wei, Jie Liu

Abstract—A new gelling material called Soil Solidification Rock (SSR), based on industrial waste and discarded concrete, dramatically reduces the negative impacts of the concrete preparation process and offers significant advantages in terms of energy consumption and material costs. The freezing resistance and microstructure of concrete with 70% and 100% (9%, 12%, and 15%) SSR content were investigated by freeze-thaw cycle tests and scanning electron microscopy organization. The study results indicated that the frost protection of concrete was significantly improved after reinforcing recycled aggregates with cement silica fume mortar. As the SSR admixture increased from 9% to 12% and 15%, the relative dynamic resilient modulus of concrete was significantly increased after a similar number of freeze thaw cycles, while the mass loss rate was significantly reduced. It is significant that the crushing strength of RAC cured with 70% SSR even exceeds that of Recycled Aggregate Concrete (RAC) cured with 100% SSR after freeze-thaw cycles. In addition, the surface-treated SSR-cured RAC showed a significant enhancement in the freezing resistance index (DF). Compared to the untreated control group, the cement-silica fume-treated group of geodesic cured recycled aggregate concrete was able to withstand a greater frequency of freeze-thaw cycles, indicating that the frost resistance of the concrete was enhanced accordingly with the elevated geodesic admixture.

Index Terms—Soil Solidification Rock, Recycled Concrete Aggregate, durability, Microscopic test

I. INTRODUCTION

AS urbanization and economic development accelerate globally, the generation of large quantities of CDW has

caused serious negative impacts on the environment^[1,2]. C&D wastes are directly dumped in landfills, causing environmental damage and resource wastage^[3,4]. In addition, the strong demand for natural aggregates (NCA) has led to over-exploitation and accelerated the acute shortage of quality sand and gravel^[5,6]. The utilization of Recycled Concrete Aggregates (RCA) as an alternative to natural stone for the production of RAC is an effective way for sustainable development^[7]. Recycled aggregates are environmentally friendly and facilitate easy recycling^[8]. Utilizing waste concrete as RCA reduces carbon emissions by approximately 15-20%^[9] and decreases the consumption of limestone resources by roughly 60%^[10]. RCA has found widespread application in asphalt pavements^[11], building structures^[12], and sidewalks^[13] across numerous countries, including the United States and China.

The utilization of RCA confers environmental benefits by conserving resources and diminishing pollution; however, it is associated with drawbacks such as increased porosity, elevated water absorption, and a compromised Interface Transition Zone (ITZ)^[14]. In regions subject to freezing and thawing cycles, concrete structural degradation is a prevalent issue^[15]. After such cycles, the ITZ in RAC is susceptible to the development of microcracks, leading to a reduction in bond strength and compromising the structural integrity and longevity^[16]. Qian Huixiao's study^[16] examined the durability of RAC when exposed to a dual attack of freeze-thaw cycles and sulfate exposure, noting that aggregate substitution rates above 50% could lead to a substantial decline in frost resistance, potentially falling short of frost resistance criteria. Yao Yizhou's research^[17] delved into the degradation mechanisms of Reactive Powder Concrete (RPC) under the concurrent influence of sulfate attack and freeze-thaw cycling, highlighting that the distribution and quality of recycled aggregates significantly influenced the extent of damage to RPC. Ji Yongcheng^[18] systematically investigated the mechanical damage mechanism of recycled brick RAC under freeze-thaw cycling conditions by using experimental and finite element modeling methods. Mohammad Saberian^[19] evaluated the effectiveness of freeze-thaw cycling in roadbed subgrade.

In the construction industry, cement has long served as a fundamental binding material. However, its production demands considerable energy and results in significant carbon dioxide emissions, posing environmental challenges that are at odds with China's sustainable development goals. In contrast, SSR emerges as a promising alternative—an

Manuscript received August 18, 2024; revised December 26, 2024.

The work is supported by financial grants from the Natural Science Foundation of Shandong Province (ZR2023QE205).

Jianjun Teng is a manager of the Shandong Expressway Construction Management Group Co., China (e-mail: tjjslb@163.com).

Nan Shi is a manager of Shandong Expressway Yampong Highway Co., China (e-mail: 0531shinan@163.com).

Haifeng Wan is a professor of Engineering of Yantai University, China (corresponding author to provide phone: 13181632592; e-mail: ytuwan@126.com).

Yangfan Xin is a manager of Shandong Expressway Yampong Highway Co., China (e-mail: xinyangf@126.com).

Cheng Jin is a postgraduate student of engineering of Yantai University, China (e-mail: 862286579@qq.com).

Jie Wang is a manager of Shandong Expressway Yampong Highway Co., China (e-mail: 18668906083@163.com).

Zuwei Liu is a professor of Engineering of Yantai University, China (e-mail: liuzuwei@ytu.edu.cn).

Huijie Wei is a postgraduate student of engineering of Yantai University, China (e-mail: 1752575832@qq.com).

Jie Liu is a manager of the Shandong Expressway Construction Management Group Co., China (e-mail: 2579783055@qq.com).

innovative, low-carbon, environmentally friendly material crafted from industrial solid wastes such as steel slag, fly ash, red mud, and coal gangue^[20,21]. Red mud is usually disposed of by burying it on-site or dumping it into the ocean, and a large amount of heavy metal elements in red mud seriously pollutes the environment^[22]. Coal gangue is a solid waste generated during mining and processing^[23]. Developed through a clean preparation process based on geological principles, soil tuff matches the strength and structural suitability of cement while offering a reduced environmental footprint^[24]. SSR can manage these CDW, while offering advantages such as mechanical strength, water stability, frost resistance, high-temperature resistance, and corrosion resistance. SSR effectively leverages on-site resources, minimizes the extraction and use of natural materials, and reduces carbon emissions, thereby showcasing strong sustainability. Furthermore, since the ITZ of RAC is very complex, the destruction mechanism of SSR RAC in freeze-thaw (F-T) environments is not clear and needs to be further explored.

Current research on recycled aggregate concrete piles in cold regions, which utilize SSR as a cementing material, is limited. Studies on the optimal dosage of SSR and the mechanisms of microstructural damage after freeze-thaw cycles are particularly scarce. This paper addresses this gap by investigating recycled concrete prepared with reclaimed aggregate, reinforced with SSR at 9%, 12%, and 15%, and with a cement replacement rate of 70% to 100% using wollastonite. The freeze-thaw resistance of the RAC was assessed based on the observable characteristics of the concrete specimens, as well as the related Rapid Elastic Deformation Modulus (REDM) and Mass Loss Ratio (MLR). Additionally, the study evaluated the mechanical properties through compressive strength tests and SEM, analyzing the surface degradation of RAC after exposure to freeze-thaw cycles. The research aimed to clarify the degradation mechanisms of recycled conventional concrete under cyclic freeze-thaw conditions and to enhance the performance and cost-effectiveness of its mix design. The findings provide substantial guidance for engineering design and construction practices in cold regions, thereby contributing to the development of sustainable and resilient infrastructure.

II. RESEARCH SIGNIFICANCE AND STRATEGY

In this study, an in-depth exploration of frost durability and microscopic properties of recycled aggregate concrete (RAC) with 70% and 100% admixtures cured with different dosages of SSR (9%, 12%, and 15%) has been conducted. The recycled aggregate surface treatment technique was incorporated, and freeze-thaw cycling tests and scanning electron microscopy (SEM) analyses using the quick-freeze method were employed. Quality loss ratios, comparative modulus of kinetic elasticity, and scanning electron microscopy tests were carried out to comprehensively evaluate its performance. The results of these tests will contribute to a more profound understanding of the performance characteristics of RAC, accurately assess its frost durability, and promote the application and development of this material in cold environments. The structure of the study is presented in Figure 1.

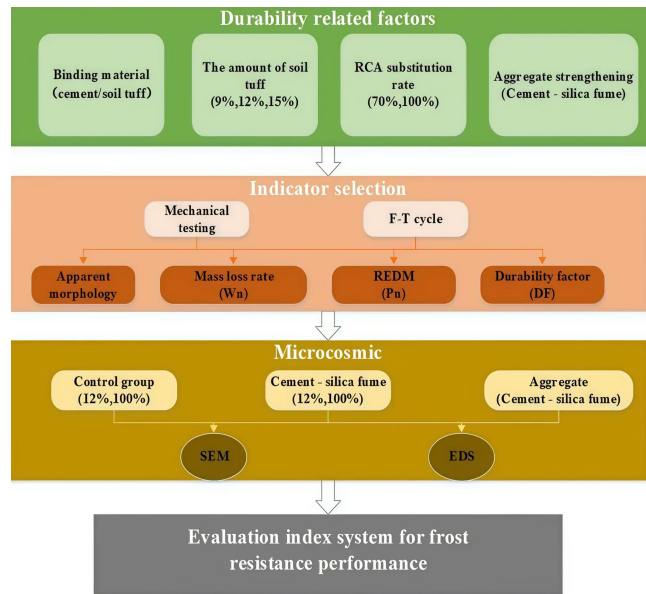


Fig. 1. Research framework of frost resistance of high content recycled aggregate solidified by SSR

III. MATERIAL AND METHODS

A. Materials

a. Gelling material

In this experiment, the gelling materials employed for concrete preparation comprised SSR. Table 1 presents the performance indexes of the gelling compounds, while Table 2 displays their chemical compositions. SSR is a silicon-calcium system gelling material produced from industrial solid wastes such as steel slag, fly ash, and coal gangue. These wastes are treated with lithogenic agents through a special preparation process. Among them, steel slag, fly ash and gangue were mixed in the same amount, and one-tenth mass fraction of exciter was also used as an admixture. The XRD analysis diagram of SSR shown in Fig. 2 was obtained by using the microscopic method of X-ray diffraction to analyze the composition of SSR. Through this analysis, it can be understood that the main mineral components in SSR are calcite, quartz, and calcium magnesium aluminum silicate.

TABEL 1
PERFORMANCE INDEX OF GELLING MATERIALS

Material types	Den sity g/c m ³	Specifi c surface kg/m ²	Fine ness %	Curing time	Flexur al streng th /MPa	Compressi ve strength /MPa
SSR	≥2700	≥350	≤10	Initial ≥180min 6h ≤ Final ≤10h	7d ≥3.0 28d ≥5.5	7d ≥10.0 28d ≥30.0

TABLE 2
CHEMICAL COMPOSITION OF GELLING MATERIAL

Ingre dient	Materi al types	CaO	SiO ₂	Al ₂ O ₃	Fe ₂ O ₃	SO ₃	K ₂ O	Oth er
Mass fracti on (%)	SSR	51.61	23.92	12.78	3.23	2.23	1.14	5.09

The granularity distribution of SSR and cement is clearly depicted in Fig. 3. From the particle size distribution of SSR, it is obvious that the particles are mainly concentrated around 20 μm. Additionally, there are a small number of small particles below 0.4 μm and large particles close to 200 μm, with a low bulk density. The bulk size concentration of SSR is more homogeneous, featuring more small and large particles. This contributes to the enhancement of contact points and interlocking effects between the particles, thereby improving the bonding capacity and strength. In contrast, the size profile in cement is more concentrated, and the difference in particle size is not as pronounced as in SSR. Consequently, cement is not as good as SSR in terms of bonding capacity and strength.

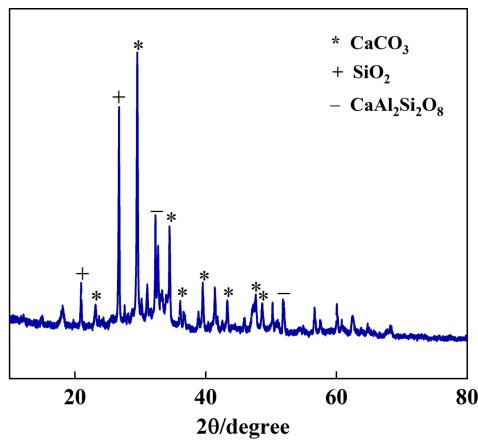
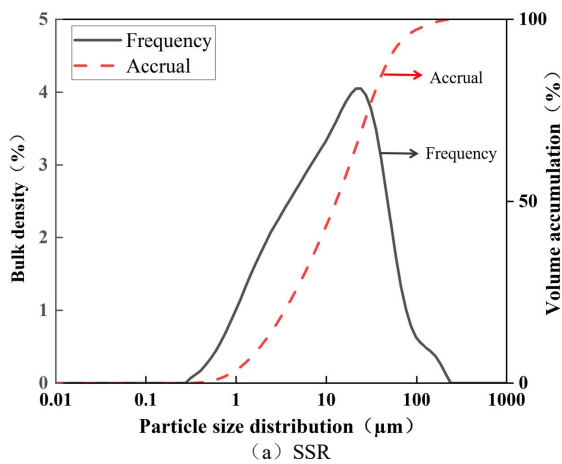
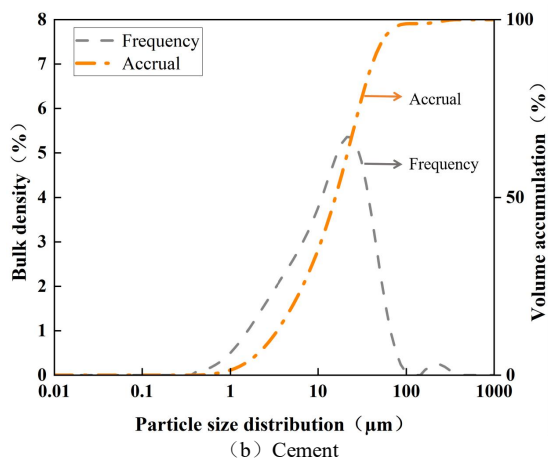


Fig. 2. XRD analysis of SSR



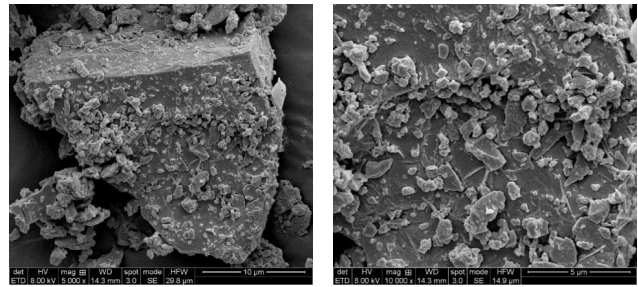
(a) SSR



(b) Cement

Fig. 3. Particle Size Distribution

Fig. 4 presents the SEM images of SSR at magnifications of 5000 and 10000 times. It contains various mineral particles, pores, hydration products, and so on. The surface structure of SSR has more particles and more pores between the particles. SSR particles exhibit a variety of morphologies, including massive, pointed, rhomboid, and spherical. The particle size varies greatly, but the overall particle size distribution is relatively uniform. As a gelling material, SSR particles of different sizes can effectively fill the gap of aggregate and enhance the cementation ability.



(a) 5000 times (b) 10000 times
Fig. 4. Scanning Electron Microscope Image of SSR

b. Aggregate

The physical properties of the coarse aggregates employed in the experiment are presented in Table 3. Silica fume is formed by the oxidation and condensation of SiO₂ and Si gases during the smelting of ferrosilicon and industrial silicon. Silica fume fills the holes between cement particles and gels with the hydrochemical products.

TABLE 3
PHYSICAL INDEX OF RECYCLED AGGREGATE

	Water absorption rate/%	Water absorption rate/%	Water absorption rate/%
NAC	2740	3.1	7.9
RAC	2568	5.4	15.6
CS-RAC	2597	6.9	10.8

B. Mix Proportion

In this paper, the SSR dosage was selected as 9%, 12%, and 15%, and the substitution rates of recycled rough aggregate were 70% and 100%, as shown in Table 4, the fits are as follows: TWR denotes the unreinforced recycled aggregate with SSR as the gelling material, TR denotes the recycled aggregate reinforced with cement silica fume with SSR as the gelling material; TR-a-b denotes the RAC reinforced with cement silica fume with SSR as the gelling material. a denotes recycled aggregate substitution rate (%), b denotes SSR admixture (%).

TABLE 4
MIX PROPORTION OF CONCRETE SAMPLE

Number	Soil tuff /kg·m ⁻³	Sand /kg·m ⁻³	Aggregates /kg·m ⁻³		Water /kg·m ⁻³
			Natural	Recycled	
TWR-100-12	287	873	0	1004	163
TR-70-9	215	924	358	767	123
TR-100-9	215	924	0	1096	123
TR-70-12	287	873	347	742	163
TR-100-12	287	873	0	1060	163
TR-70-15	359	822	335	717	204
TR-100-15	359	822	0	1024	204

C. Test equipment and test method

a. Mechanical property test

The mechanical property trials were conducted per JTG3420-2020^[25]. The effective length × width × height of the concrete specimens for the compressive strength test was 100 mm × 100 mm × 400 mm. Figure 5 shows the compressive test.

b. Frost resistance test

The frost resistance test was carried out using the “rapid freezing method” according to the long-term performance and durability test method in JTG3420-2020^[25]. Figure 6 indicates the freeze-thaw cycle test.

The relative dynamic modulus of elasticity is calculated as follows:

$$P = \frac{f_n^2}{f_0^2} \times 100\% \quad (1)$$

P represents the relative dynamic modulus of elasticity after n cycles (%). f_n is the transverse fundamental frequency of vibration after n cycles, in hertz (Hz). f_0 is the initial transverse fundamental frequency, in Hz. The formula for calculating the durability factor is as follows:

$$DF = \frac{PN}{M} \quad (2)$$

DF denotes the durability factor. P represents the absolute value of relative dynamic elasticity at N cycles, in percentage (%). N is the cycle number at which the test is terminated when P reaches a specified minimum value. M is the specified number of cycles to terminate the test. The rates of mass loss of concrete samples were calculated using the following formula:

$$W_N = \frac{m_0 - m_n}{m_0} \times 100\% \quad (3)$$

Where: W_0 is the initial mass of the concrete sample;

W_n is the mass of the concrete sample after n freeze-thaw cycles.

c. Microscopic test

Utilizing SEM, the microstructural characteristics of cured regenerative aggregate concrete specimens were investigated both before and following the application of freeze-thaw cycles. The analysis was conducted employing a CTESCAN CLARA ultra-high resolution FE SEM to meticulously examine the micromorphology of the concrete samples.

IV. RESULTS AND DISCUSSIONS

A. Analysis of frost resistance durability under freeze-thaw cycle

a. Mass loss rate

The quality loss curves of the conventional concrete specimens after freeze-thaw cycles are presented in Fig. 7. During the initial 50 freeze-thaw cycles, each group of concrete exhibits a negative mass loss, indicating a reduction in the quality change of concrete during this stage. However, after more than 50 cycle times, the upward trend of the quality ratio profiles slows down. Particularly during the 100 to 150 freeze-thaw cycles, the increase in quality loss rate begins to accelerate. In the subsequent 150 to 200

freezing-thawing cycles, this rate of rise increases rapidly. The mass loss rates of TR-70-9, TR-100-9, TR-70-12, TR-100-12, and TR-100-15 exceed the 5% threshold for destruction. TR-70-15 also loses more than 5% of its quality during the 200 to 250 freeze-thaw cycles, reaching a state of destruction.

As shown in Figure 7(a), when 9% SSR was added to the concrete and 70% and 100% recycled coarse aggregate (RCA) were used respectively, the trends of the curves of the two were identical before reaching the damage criterion. At this juncture, the concrete with 70% RCA exhibited a reduction in mass loss of approximately 0.6% compared to the concrete with 100% RCA. When the concrete was mixed with 12% SSR and the concrete with 70% and 100% RCA was compared again, the quality loss rate of 70% RCA was reduced by about 1.1% compared to 100% RCA at the time of reaching the damage criterion. In the case of 15% SSR, the concrete with 70% RCA showed a smoother variation in the mass loss rate curve and lower mass loss ratios.



Fig. 5. Compressive performance test



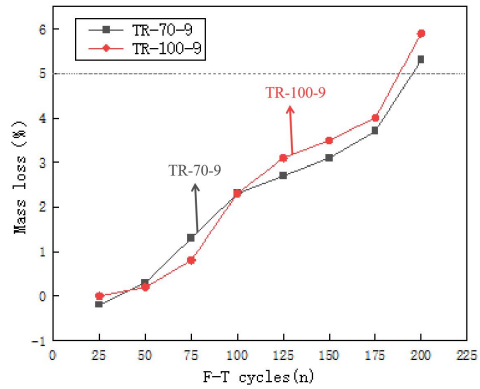
Fig. 6. Freeze-thaw cycle test

The principal source of the observed increase in specimen mass at the beginning of the freeze-thaw cycle is the occurrence of a critical volume of pores and microcracks in the specimen, offering space for the filling of the AFt and SSR hydration products. Meanwhile, during freeze-thaw cycles, free water in concrete freezes and produces an expansion effect. When this expansion exceeds the tentative force of the concrete, new miniature cracks are created inside the specimen^[26]. Quality starts to decrease within 25 freeze-thaw cycles due to the gradual expansion in microcracks leading to damages in the concrete structure, and the mass spalled from the specimens is much larger than the mass-produced by the internal reaction products, thus the mass loss rate curve shows an upward trend.

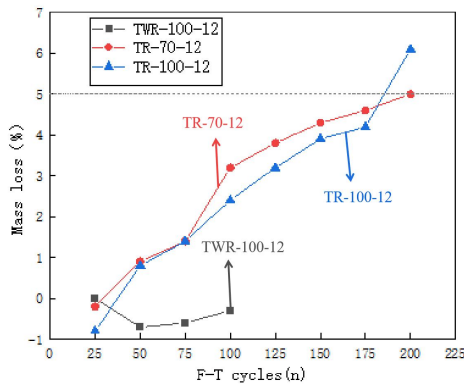
b. The Relative Dynamic Modulus of Elasticity

As depicted in Figure 8, the kinetic elastic modulus of the concretes in each group undergoes a continuous decline with the increase in the number of freeze-thaw cycles. During the initial 50 cycles, the relative dynamic elastic modulus shows a slight decrease. However, in the interval of 50 to 100 cycles, the relative dynamic elastic modulus for TWR-100-12

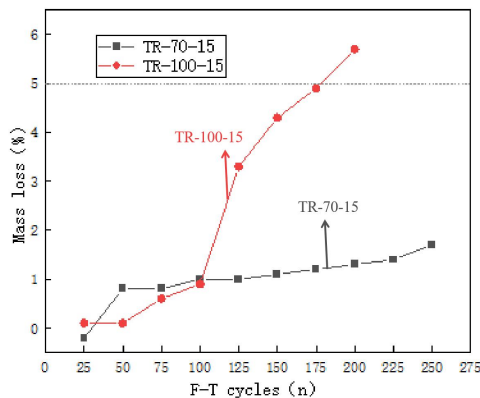
decreases significantly, dropping below 60% and indicating the onset of damage. Similar trends are observed for TR-70-15 in the 200 to 250 cycle range, where both the relative dynamic modulus of rebound and the relative dynamic modulus of resilience decline sharply, falling below the critical threshold of 60% to signify damage. By the stage of 200 to 250 frost-thaw cycles, the relative movable elastic modulus of TR-70-15 reduces at an accelerated rate, with the corresponding kinetic elastic modulus dropping below 60%, culminating in the state of destruction.



(a) 9% SSR



(b) 12% SSR

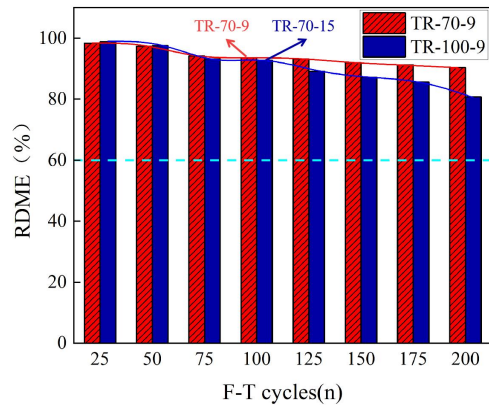


(c) 15% SSR

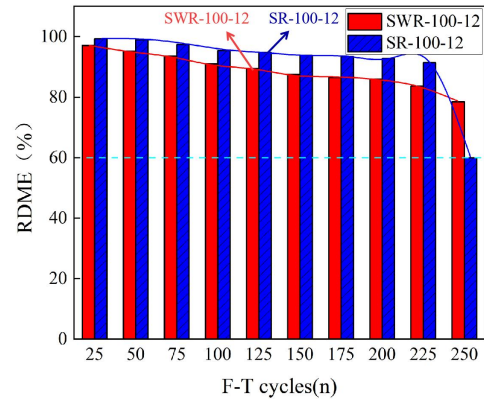
Fig. 7. Quality Loss Curve of Concrete following Freeze-Thaw Cycling

As observed in Fig. 8(a), when 9% SSR and 70% and 100% RCA were doped, the trends of the relative kinetic flexibility models were the same. Among them, the fall of relative kinetic flexibility models was relatively slower in the 70% RCA group. At the time of reaching the damage criterion, the relative kinetic flexibility model of the 70% RCA group showed an increase of 9.6% compared to that of the 100% RCA group. Fig. 8(b) shows that when 12% SSR

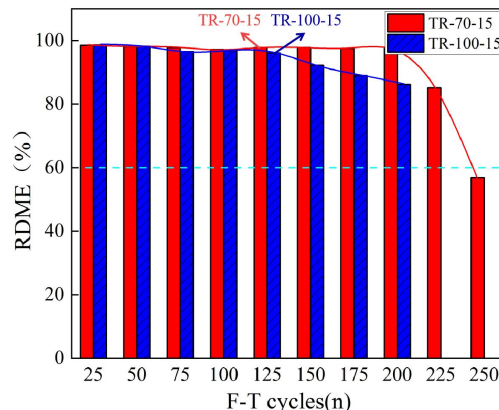
doping and 70% and 100% RCA doping were applied, the trend of relative kinetic elastic modulus was also basically the same. The TWR group decreased faster than the TR group, and the TWR group reached the damage criterion at 100 cycles. At this time, the relative kinetic elastic modulus of the 70% RCA group was improved by 0.8% compared to that of the 100% RCA group. As shown in Fig. 8(c), with the addition of 15% SSR and 70% and 100% RCA, the relative toughness modulus of the 70% RCA group changed relatively smoothly. However, it decreased rapidly after 200 cycles and reached the destruction criterion at 250 cycles. An increase in the frequency of recycled coarse aggregate substitution is associated with a reduction in the concrete's relative ductile modulus. Conversely, an increase in the proportion of SSR leads to an enhancement in the relative ductile modulus.



(a) 9% SSR



(b) 12% SSR



(c) 15% SSR

Fig. 8. Relative Dynamic Elastic Modulus of Concrete after Freeze-Thaw Cycle

There is a more pronounced attenuation trend for TR-100-12 than TR-70-12 and a more pronounced attenuation trend for TWR-100-12 than TR-100-12 under the same freeze-thaw cycle conditions. This shows that the quality of aggregates directly contributes to the frost resistance and longevity of concrete. The reason is that the cement-silica fume fills the voids of RCA. Compared with NCA and CSRAC, RCA has higher porosity, which reduces the contact area with the hydration products of SSR, and reduces the generation rate of ettringite, $\text{Ca}(\text{OH})_2$, and C-S-H, thus reducing the compactness of the specimen and RDME^[27]. However, as with the freeze-thaw cycle test, ettringite and other hydration products continue to generate and accumulate, and its expansion stress continues to rise, causing the concrete specimen to be destroyed.

c. Durability index of concrete under freeze-thaw cycle

Fig. 9 shows the ductile fortification index DF of the concretes. The DF values of all the groups of concretes showed a similar increasing trend with a relatively slow increase when the number of freeze-thaw cycles was from 0 to 50, whereas the concrete THR-100-12 was destroyed when the number of freeze-thaw cycles was 100. From 75 to 200 freeze-thaw cycles, the DF values of all groups of concrete continued to increase with the same trend, and TR-70-9, TR-100-9, TR-70-12, TR-100-12, and TR-100-15 were damaged at 200 freeze-thaw cycles. The values of TR-70-15 DF show a decreasing trend from 200 to 250 cycles. TR-70-15 fails at 250 cycles. Thus, the DF of cement-silica fumed SSR-cured highly doped RAC is greatly enhanced compared to that of SSR-cured highly doped RAC without surface treatment.

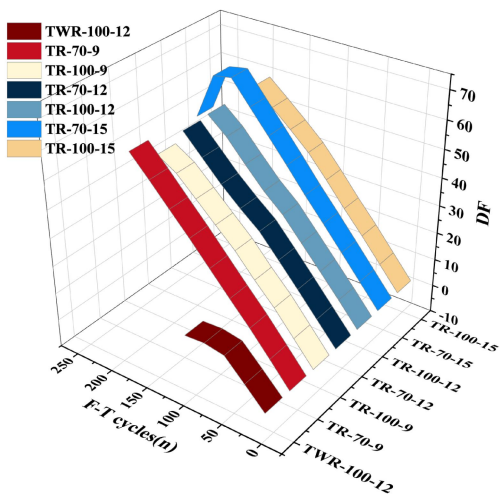


Fig. 9. Antifreeze Durability Index DF

d. Damage state of concrete sample surface under freeze-thaw cycle

Figure 10 illustrates the progressive degradation of concrete specimens subjected to a freeze-thaw cycle protocol^[25]. Focusing on TR-70-15, spalling initiated in the surface-applied SSR paste is observed after 100 cycles, evident by the development of small holes and a decrease in surface evenness. Upon increasing the cycle count to 200, the specimen's surface becomes notably pitted, with fine aggregates becoming exposed and detached, creating a surface morphology resembling craters. After 250 passes, the

graded surfaces became more devoid of air and the surfaces were severely damaged. 100% recycled coarse aggregate specimens showed the most severe freeze-thaw damage due to microcracking of the recycled aggregate during crushing and the old grout adhering to the edges of the surfaces, which resulted in the most severe freeze-thaw damage to the specimens. The coarse aggregate on the surface of the specimen was exposed. After 100 cycles, the mortar on the surface of the unsurfaced concrete was dislodged in large quantities, and the surface-treated concrete could only achieve the same damage effect after 200 cycles, which was since the surface of the recycled aggregate was coated with a layer of cement-silica fume mortar, and the average particle size of silica fume was about 1/100 of the cement particles^[28].

Specimen	0 freeze-thaw cycle	100 freeze-thaw cycle	200 freeze-thaw cycle
TR-70-9			
TR-70-12			
TR-70-15			
TR-100-9			
TR-100-12			
TR-100-15			
TWR-100-12			

Fig. 10. Apparent state of freeze-thaw cycle damage process of specimen

B. Mechanical property test under freeze-thaw cycle

a. Compression failure mode of concrete samples before and after freeze-thaw

Figure 11 shows the compression damage pattern of the specimens before and post freeze-thaw cycles. As the pressure is gradually increased, these cracks will gradually propagate toward the center of the specimen, during which the concrete will gradually spill. When the final failure load is reached, the sample will produce oblique through cracks, resulting in the concrete sample being divided into two pieces of different sizes, and its integrity will be damaged. After freeze-thaw cycle, there are many small vertical cracks appearing on the test specimen surface at the initial phase of compression, and the concrete is gradually spalled off. Consequently, massive cracks are produced in the middle of the specimen and the spalling of the surrounding concrete is intensified with the gradual increase in pressure. When the final failure load is reached, oblique through cracks are produced, and the damage of one end of the sample is obvious, and the integrity is damaged^[29].

b. Mechanical properties under freeze-thaw cycles

The technical specifications of the compressive strength of concrete specimens before and after freeze-thaw cycles are illustrated in Table 5 and Fig. 12. From Fig. 12, it can be seen that the strength of untreated SSR RAC is 9 MPa while the compressive strength of cement-silica fume-treated SSR

RAC is 20 MPa. Table 5 shows that the residual strength ratios of RAC with 70% substitution are generally higher than those of RAC with 100% substitution. The residual strength ratios of TR-100-9, TR-100-12, and TR-100-15 are 50%, 60%, and 63.64%, respectively.

C. Analysis of micro test results

a. SEM Test Results of Recycled Aggregate

Fig. 13 reveals scanning electron microscope images of the surface of the renewable aggregate and the reinforced pre-reinforced recycled aggregate. From Fig. 13(a), it is clear that the surface of the recycled aggregate is covered by a large amount of hardened mortar, and the surface of the aggregate is uneven. From Fig. 13(b), it is clear that the surface of the recycled aggregate is covered with hardened mortar and has a loose structural organization together with a considerable number of pores, resulting in high water absorption, low density, and relatively low strength.

Fig. 14 is an SEM image obtained from the reinforced recycled aggregate surface. From Fig. 14(a), it is evident that the surface morphology of the cement-silica fume-treated recycled aggregate is denser than that of an untreated reclaimed aggregate, and the reinforced treated recycled aggregate has a crystalline skeleton structure. From Fig. 14(b), it can be seen that the hydration products of cement and silica fume were on the interface of renewed aggregate and filled the voids, which improved the inter-facial denseness and bonding capacity.






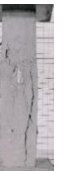






Specimen	TR-70-9	TR-70-12	TR-70-15	TR-100-9	TR-100-12	TR-100-15
Original specimen						
Specimen after freeze-thaw cycle damage						

Fig. 11. Compression failure mode of the sample before and after freeze-thaw damage

TABLE 5
TECHNICAL INDEXES OF COMPRESSIVE STRENGTH OF CONCRETE SAMPLES BEFORE AND AFTER FREEZE-THAW CYCLE

Specimen number	Compressive strength before freezing and thawing (MPa)	Compressive strength after freezing and thawing (MPa)	Residual strength ratio (%)
TR-70-9	14	13	92.86
TR-70-12	17	14	82.35
TR-70-15	27	21	77.78
TR-100-9	20	10	50.00
TR-100-12	20	12	60.00
TR-100-15	22	14	63.64
TWR-100-12	9	8	88.89

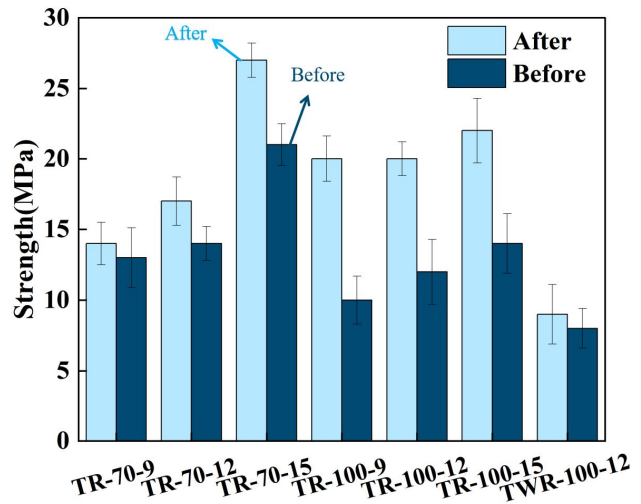


Fig. 12. Technical Indexes of Compressive Strength of Concrete Samples Before and After Freeze-Thaw Cycle

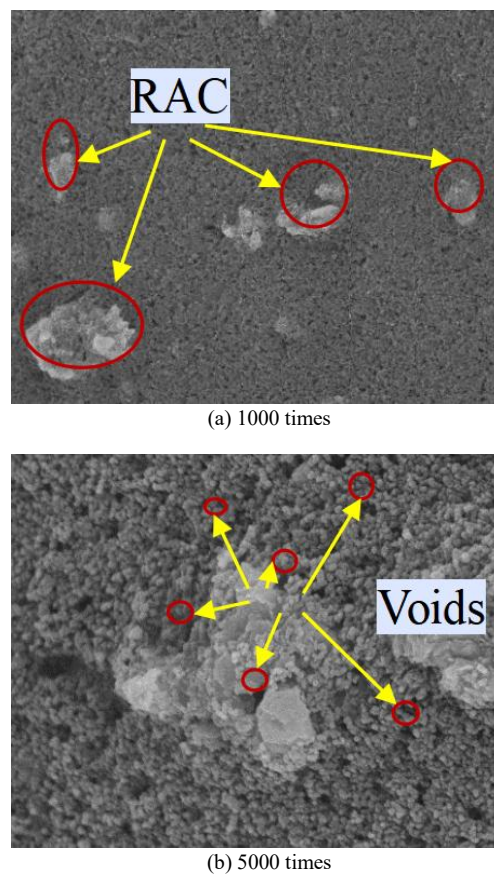


Fig. 13. SEM before reinforcement of recycled aggregate

Figs. 15(a) and (b) are the EDS diagrams of the recycled aggregate before and after the cement-silica fume treatment. Comparing the results before and after treatment, the contents of Ca, Si, and S increased significantly. The total increase is 52%, and the content of calcium is also significantly increased by 83%, which indicates that a large amount of calcium silicate is generated on the surface of the treated aggregate to fill the tiny cracks and pores of the aggregate. Firstly, it augments the inherent strength of recycled aggregates and mitigates stress concentration arising from internal defects. Secondly, filling the pores prevents the infiltration of external erosive substances such as water and chloride ions, thus enhancing the durability of recycled aggregates. This enhanced durability ensures their effective

utilization in construction engineering.

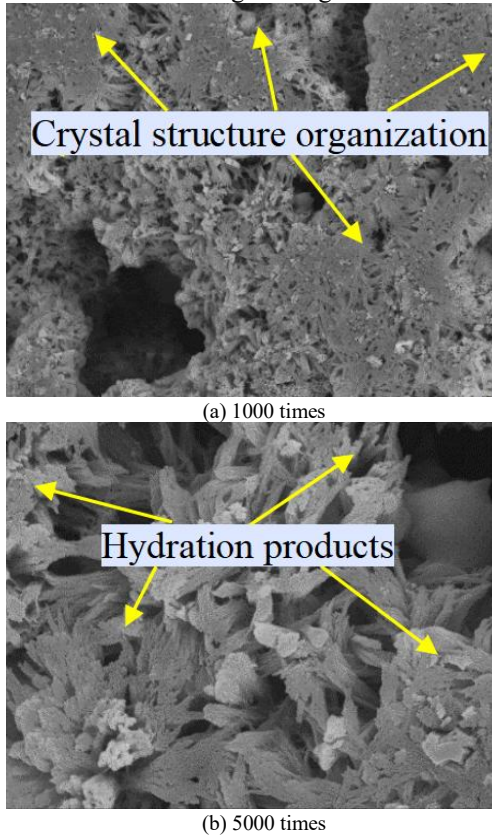


Fig. 14. SEM after reinforcement of recycled aggregate

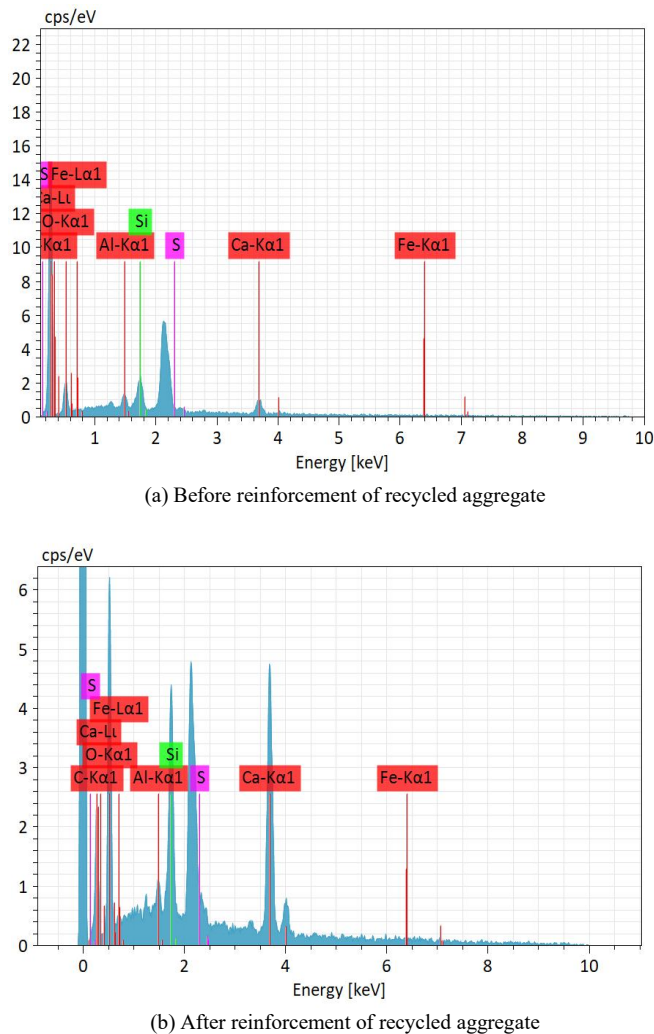


Fig. 15. EDS Diagram of Recycled Aggregate

b. Analysis of concrete SEM test results

Specimen	Original specimen	Specimen after freeze-thaw cycle damage
1000 magnification		
2000 magnification		
1000 magnification		

Fig. 16. SEM images of recycled concrete before and after freeze-thaw cycle

Figure 16 shows the SEM images of recycled concrete before and after freeze-thaw cycles. Before the freeze-thaw cycle, the SSR underwent a full hydration reaction with water, generating a large number of gel products, such as C-S-H, C-A-H, and so on. In addition, SSR is rich in reactive SiO₂ and Al₂O₃ and other silica-aluminum mineral components, which are activated by alkali excitation during the hydration process, and undergo earth polymerization reactions such as ionic bond breaking, depolymerization, and condensation, generating flocculated C-A-S-H. Part of the hydrated gel is wrapped up and fills the pores between the discrete aggregates to form agglomerates, which effectively reduces the internal porosity and significantly improves the matrix densification. This effectively reduces the internal porosity and significantly increases the matrix densification. The remaining gel forms an external support skeleton after solidification and hardening, connecting the discrete agglomerates. Large freezing force after the freeze-thaw cycle, hydrated calcium silicate gel is relatively intact, but cracks are produced in the inter-facial transition zone. SSR hydrate is detached from the aggregate, accompanied by the emergence of tiny cracks, and the formation of needle-like calcium alumina. The RAC is seriously damaged, and tortoise cracks are produced. The cracks penetrate through the interface and extend from the inter-facial transition zone to the periphery, and the SSR slurry spalls seriously. The water absorption of recycled aggregate is large, and the RAC is susceptible to freeze-thaw erosion. The old mortar with recycled aggregates has holes penetrating from the inside to the outside, which are dense and numerous, and a small amount of needle-like calcite erosion products. During

freeze-thaw cycling, water gradually penetrates into the interior of the concrete and freezes ice resulting in an increase in volume and a decrease in volume upon thawing, generating cyclic stresses. Whether or not the interior of the concrete can remain intact depends on the magnitude of the freeze-thaw cyclic tensile stress and the tensile stress that the concrete itself can withstand. The incorporation of RCA leads to a reduction in freezing resistance compared to NCA. The presence of old adherent mortar on the surface of the RCA and internal cracked pores provides a poorer ITZ for bonding with aggregates and poorer bonding with the new mortar. This results in RCA absorbing water and creating expansive tensile stresses during freeze-thaw cycles and not being able to withstand the higher stresses applied.

V. CONCLUSIONS

In this paper, cement silica fume was employed as a reinforcing material to enhance the performance of RAC. The frost resistance and micro-mechanisms of RAC cured with different admixtures (9%, 12%, 15%) and high contents (70%, 100%) of SSR were investigated, including mechanical properties, mass-loss rate, relative kinetic-elastic modulus, and SEM. Based on the consequence analysis, the following conclusions can be drawn:

(i) For the same amount of SSR, concrete with a lower percentage of RCA (70%) has a lower mass loss than concrete with a higher percentage of RCA (100%), ranging from 0.6% to 1.1%. The appropriate amount of SSR and RCA can effectively enhance the freeze-thaw resistance of concrete. Meanwhile, cement silica fume mortar reinforced with RCA can effectively increase the apparent density of concrete and improve the frost resistance of RAC.

(ii) An increase in the SSR content from 9% to 15% was found to be accompanied by a corresponding increase in the production of hydration gels. This resulted in a significant improvement in void-filling efficacy and a richer and more robust bonding and skeletal structure within the hydration by-products. Concretes subjected to freeze-thaw cycles showed a 6.2% increase in relative dynamic modulus of elasticity and a 4% reduction in mass loss rate, indicating a profound enhancement in the frost durability of the materials.

(iii) Under the same freeze-thaw cycle conditions, concrete with 12% SSR and 100% recycled coarse aggregate reduces the relative dynamic modulus of elasticity by approximately 9.6% compared to concrete with 9% SSR and 70% recycled coarse aggregate.

(iv) The residual strength ratios of RAC cured with 70% SSR were higher than those of RAC cured with 100% soil, indicating that proper addition of RCA can improve the structural stability and ductility of concrete. The frost durability index (DF) of SSR-cured RAC with cement-silica fume treatment was significantly higher than that of SSR-cured RAC without surface treatment. The cement-silica fume treatment was effective in improving the performance of RCA and enhancing the durability of RAC in low-temperature environments.

(v) Upon completion of 100 freeze-thaw (FT) cycles, the specimens without additional reinforcement exhibited failure. This failure threshold was similarly reached in specimens containing 9% and 12% SSR as well as in the TR-100-15 concrete after 200 FT cycles. The TR-70-15 specimens

within the treated group failed at 250 cycles. The number of FT cycles leading to failure was predicted using the Weibull distribution, with values of 78 for TWR-100-12 and 287 for TR-100-12. The SSR-cured RAC treated with a blend of cement and silica fume showed a significant enhancement in frost resistance, in contrast to the poor frost performance of untreated SSR-cured RAC. Additionally, an increase in SSR content was found to be associated with an improvement in the frost resistance of RAC.

In general, the treatment of RCA with cement and silica fume can effectively improve the mechanical properties and microscopic characteristics of RAC. This study focused on the effects of SSR dosage and recycled aggregate content on SSR-cured high-content RAC. It analyzed the performance of the concrete in a freeze-thaw environment and provided a series of research results with practical value, guiding the application of SSR-cured high-content RAC in cold regions. These results will help to promote the application of high-volume recycled concrete in practical engineering and improve the sustainability and durability of concrete structures.

VI. SUGGESTIONS FOR FUTURE RESEARCH

The recommendations for future research on this topic are set out below:

(i) The fatigue performance of reconditioned aggregate concrete made of reinforced concrete under repeated dynamic loading directly affects the service life of civil engineering structures. Future research should strengthen the experimental study on the fatigue life span at different stress ratios and loading frequencies of recycled aerial concrete made of reinforced concrete, and establish the fatigue equation of recycled aerial concrete made of reinforced concrete.

(ii) There is still room for improvement in the mechanical properties of RAC cured with SSR. We should develop a new generation of RAC by adding fibers, nanopowders, and other technologies to expand the application of SSR-cured RAC to roads, bridges, tunnels, water conservancy projects, and other fields.

(iii) The long-term service performance of reinforced recycled aggregate concrete with reinforced concrete should be verified through practical engineering applications, and health monitoring and monitoring of concrete structures during operation are necessary.

REFERENCES

- [1] J. Jiang, H. Yang, Z. Deng, Z. Li, Bond performance of deformed rebar embedded in recycled aggregate concrete subjected to repeated loading after freeze-thaw cycles, *Constr. Build. Mater.* 318 (2022), 125954.
- [2] Li Y, Kaikai Jin, Lin H, et al. Analysis and prediction of freeze-thaw resistance of concrete based on machine learning[J]. *Materials Today Communications*, 2024, 39: 108946.
- [3] Huo Y, Qiu J, Feng Z, et al. Acoustic emission characteristics of recycled brick-concrete aggregate concrete under freeze-thaw-load coupling action and damage constitutive model[J]. *Journal of Building Engineering*, 2023, 79: 107930.
- [4] Ma F, Zhang Y, Qiao H, et al. Analysis of damage models and mechanisms of mechanical sand concrete under composite salt freeze-thaw cycles[J]. *Construction and Building Materials*, 2024, 429: 136311.
- [5] Liu K, Yan J, Zou C. A pilot experimental study on seismic behavior of recycled aggregate concrete columns after freeze-thaw cycles[J]. *Construction and Building Materials*, 2018, 164: 497-507.

- [6] Liu K, Yan J, Meng X, et al. Bond behavior between deformed steel bars and recycled aggregate concrete after freeze-thaw cycles[J]. *Construction and Building Materials*, 2020, 232: 117236.
- [7] A. Gholizadeh-Vayghan, A. Bellinkx, R. Snellings, B. Vandoren, M. Quaghebeur, The effects of carbonation conditions on the physical and microstructural properties of recycled concrete coarse aggregates, *Constr. Build. Mater.* 257 (2020), 11948.
- [8] Wang W, Wang Y, Chen Q, et al. Bond properties of basalt fiber reinforced polymer (BFRP) bars in recycled aggregate thermal insulation concrete under freeze-thaw cycles[J]. *Construction and Building Materials*, 2022, 329: 127197.
- [9] H. Guo, C. Shi, X. Guan, J. Zhu, Y. Ding, T.C. Ling, H. Zhang, Y. Wang, Durability of recycled aggregate concrete – A review, *Cem. Concr. Compos.* 89 (2018) 251–259.
- [10] Hui L ,Xudong Z ,Pinghua Z , et al. Carbonation treatment to repair the damage of repeatedly recycled coarse aggregate from recycled concrete suffering from coupling action of high stress and freeze-thaw cycles[J]. *Construction and Building Materials*, 2022, 349
- [11] Nwakaire M C ,Yap P S ,Yuen W C , et al. Laboratory study on recycled concrete aggregate based asphalt mixtures for sustainable flexible pavement surfacing[J]. *Journal of Cleaner Production*, 2020, 262
- [12] Lin Y, Zhang Z, Feng X. Three-dimensional microstructural simulation of the thermodynamic behavior of recycled concrete under freeze-thaw action[J]. *Journal of Building Engineering*, 2023, 80: 108099.
- [13] Adebayo Ibrahim, Utilisation of recycled concrete aggregates for sustainable highway pavement applications; a review, *Constr. Build. Mater.* 235 (2020) 117444.
- [14] Jiang J, Yang H, Deng Z, et al. Bond performance of deformed rebar embedded in recycled aggregate concrete subjected to repeated loading after freeze-thaw cycles[J]. *Construction and Building Materials*, 2022, 318: 125954.
- [15] Y. Huang, T. Wang, H. Sun, C. Li, L. Yin, Q. Wang, Mechanical properties of fibre reinforced seawater sea-sand recycled aggregate concrete under axial compression, *Constr. Build. Mater.* 331 (2022), 127338.
- [16] Qian Hui Xiao Q H, Cao Z Y, Guan X, et al. Damage to recycled concrete with different aggregate substitution rates from the coupled action of freeze-thaw cycles and sulfate attack[J]. *Construction and Building Materials*, 2019, 221: 74-83.
- [17] Yao Y, Liu C, Liu H, et al. Deterioration mechanism understanding of recycled powder concrete under coupled sulfate attack and freeze-thaw cycles[J]. *Construction and Building Materials*, 2023, 388: 131718.
- [18] Ji Y, Pei Z, Xu W, et al. Deterioration performance analysis of recycled brick concrete subjected to freezing and thawing effect[J]. *Case Studies in Construction Materials*, 2024, 20: e02722.
- [19] Saberian M, Li J. Effect of freeze-thaw cycles on the resilient moduli and unconfined compressive strength of rubberized recycled concrete aggregate as pavement base/subbase[J]. *Transportation Geotechnics*, 2021, 27: 100477.
- [20] Good F T, Kuhlman K L, LaForce T C, et al. Analytical solution and parameter estimation for heat of wetting and vapor adsorption during spontaneous imbibition in tuff[J]. *International Journal of Heat and Mass Transfer*, 2023, 203: 123814.
- [21] Capra G F, Duras M G, Vacca S, et al. Issues concerning soils treated with wastewater: Pedotechnical management with zeolitized tuffs as an option for turning N and P pollutants into potential fertilizers[J]. *Microporous and mesoporous materials*, 2013, 167: 22-29.
- [22] Wang M, Liu X. Applications of red mud as an environmental remediation material: A review[J]. *Journal of Hazardous Materials*, 2021, 408: 124420.
- [23] Shuang Shao, Baozhong Ma, Chengyan Wang, et al. Thermal behavior and chemical reactivity of coal gangue during pyrolysis and combustion[J]. *Fuel*, 2023, 331: 125927.
- [24] Huang T, Zhang S W, Zhou L, et al. Self-cementation of the alkali-activated volcanic tuff coupling with thiol-functionalized expanded perlite that enhances the solidification and stabilization of the mercury-contaminated soil[J]. *Chemical Engineering Journal*, 2022, 428: 131059.
- [25] JTG 3420-2020, Test code for cement and cement concrete in highway engineering [S].
- [26] ASTM C 666-2015, Test Method for Resistance of Concrete to Rapid Freezing and Thawing [S].
- [27] Y. Yao, C. Liu, H. Liu, W. Zhang, T. Hu, Deterioration mechanism understanding of recycled powder concrete under coupled sulfate attack and freeze-thaw cycles, *Construct. Build. Mater.* 388 (2023), 131718.
- [28] S. Jadon, S. Kumar, Stone dust and recycled concrete aggregates in concrete construction: an efficient way of sustainable development, *Proceedings, Materials Today*, 2023.
- [29] D. Xie, R. Zhang, J. Wang, The influence of environmental factors and precipitation precursors on enzyme-induced carbonate precipitation (EICP) process and its application on modification of recycled concrete aggregates, *J. Clean. Prod.* 395 (2023), 136444.
- [30] K.M. Liew, A.O. Sojobi, L.W. Zhang, Green concrete: prospects and challenges, *Constr. Build. Mater.* 156 (2017) 1063–1095.
- [31] J. Wu, X. Jing, Z. Wang, Uni-axial compressive stress-strain relation of recycled coarse aggregate concrete after freezing and thawing cycles, *Construct. Build. Mater.* 134 (2017) 210–219.